Editors' Suggestion

Observation of Efficient Lower Hybrid Current Drive at High Density in Diverted Plasmas on the Alcator C-Mod Tokamak

S. G. Baek,[1,*] G. M. Wallace,[1] P. T. Bonoli,[1] D. Brunner,[1] I. C. Faust,[1,2] A. E. Hubbard,[1] J. W. Hughes,[1] B. LaBombard,[1] R. R. Parker,[1] M. Porkolab,[1] S. Shiraiwa,[1] and S. Wukitch[1]
[1]MIT Plasma Science and Fusion Center, Cambridge, Massachusetts 02139, USA
[2]Max Planck Institute for Plasma Physics, Munich, Bavaria 85748, Germany

(Received 9 April 2018; revised manuscript received 22 June 2018; published 3 August 2018)

Efficient lower hybrid current drive (LHCD) is demonstrated at densities up to $\bar{n}_e \approx 1.5 \times 10^{20}$ m^{-3} in diverted plasmas on the Alcator C-Mod tokamak by operating at increased plasma current—and therefore reduced Greenwald density fraction. This density exceeds the nominal "LH density limit" at $\bar{n}_e \approx 1.0 \times 10^{20}$ m^{-3} reported previously, above which an anomalous loss of current drive efficiency was observed. The recovery of current drive efficiency to a level consistent with engineering scalings is correlated with a reduction in density shoulders and turbulence levels in the far scrape-off layer. Concurrently, rf wave interaction with the edge and/or scrape-off-layer plasma is reduced, as indicated by a minimal broadening of the wave frequency spectrum measured at the plasma edge. These results have important implications for sustaining steady-state tokamak operation and indicate a pathway forward for implementing efficient LHCD in a reactor.

DOI: 10.1103/PhysRevLett.121.055001

The attractiveness of a tokamak for steady-state power production depends on demonstrating a means to efficiently generate noninductive toroidal plasma current. Of the available means, lower hybrid current drive (LHCD) is the most efficient process in which LH waves Landau damp on electrons at a relatively high parallel (along the magnetic field) phase velocity of $v_{//} \sim 3v_{te}$, where $v_{te} = \sqrt{2T_e/m_e}$. As a result, both momentum transfer and an asymmetric plasma resistivity contribute to LHCD [1,2]. For this reason, research on lower hybrid current drive has been vigorously pursued with the expectation that it will ultimately play a crucial role in attaining fully noninductive operation—augmenting the edge bootstrap current with efficient off-axis current drive and providing access to high confinement regimes with the formation of an internal transport barrier by tailoring the current profile [3].

However, one of the biggest challenges since the beginning of the LHCD experiments in the 1970s [4] has been to understand and overcome the so-called LHCD density limit—an anomalous loss of efficiency observed at a density below the classical wave accessibility limit [5]. The effect has been attributed to an anomalous wave power loss or excessive broadening in the launched wave number due to undesirable wave interactions occurring at the plasma edge, such as parametric decay instabilities [6,7]. Based on the frequency scaling of this limit behavior [4], early experiments established a rule of thumb limit of $\omega_0/\omega_{\mathrm{LH}}(0) > 2$ for efficient current drive, where ω_0 is the source frequency and $\omega_{\mathrm{LH}}(0)$ is the plasma lower hybrid frequency at the plasma center, in predicting current drive performance. Nevertheless, recent experiments on various tokamaks have exhibited poorer than expected current drive efficiencies at densities below this limit (FTU [8], Tore Supra [9], EAST [10], and Alcator C-Mod [11]). The parametric decay instability (PDI) onset, which can be considered a proxy for the anomalous efficiency loss, is found to be generally initiated when $\omega_0/\omega_{\mathrm{LH}}(0) \approx 3$ to 4.

Furthermore, a more restrictive limit was observed in diverted configurations on C-Mod. While no apparent density limit behavior was observed for inner-wall limited plasma up to the accessibility limit [12], efficient current drive was observed only up to $\bar{n}_e \approx 1 \times 10^{20}$ m^{-3} in diverted discharges, corresponding to $\omega_0/\omega_{\mathrm{LH}}(0) \approx 3.2$ with $n_e(0) \approx 1.4 \times 10^{20}$ m^{-3} and $B_t(0) = 5.4$ T. Because of this unfavorable result, experimental exploration of diverted scenarios with high bootstrap current fraction at reactor relevant densities was restricted. For those plasmas exhibiting the anomalous density limit behavior on C-Mod, increasing the edge pedestal temperature up to 1 keV resulted in only a modest improvement of the current drive efficiency [12]. This was in clear contrast to results obtained from a limiter configuration on FTU [8]: the regime of effective current drive was reported to be extended with the increase in edge temperature associated with special wall conditioning and pellet injection. A key difference between the diverted and limited configurations is the behavior of the scrape-off layer (SOL), whose impact on wave propagation was not carefully examined until recently [11]. In a reactor, a divertor configuration will most likely be required in order to accommodate the

extreme levels of heat and particle exhaust. Therefore, it is crucial to determine if an approach may exist to extend the compatibility of efficient LHCD to diverted scrape-off layers operating at reactor level densities.

In the course of our research on C-Mod [13–15], we came to realize that diverted plasmas which showed this limit behavior typically had plasma currents set at a low value ($I_p < 1$ MA). The aim of choosing the low current was to maximize the noninductive current fraction due to LHCD. On the other hand, from tokamak boundary physics [16], it is known that SOL plasmas exhibit broad shoulders and increased levels of blobby turbulence at low plasma current, particularly when the Greenwald density fraction [$\bar{n}_e/n_G$, where $n_G = I_p/(\pi a^2)$] is greater than $\bar{n}_e/n_G \approx 0.2$. From the wave physics point of view, these edge conditions have recently been identified to cause a number of parasitic interactions with the boundary plasma. For example, by doubling the plasma current (0.55 → 1.1 MA) [13] and reducing the density in the far SOL by about half, parasitic wave interaction was found to be reduced with a concurrent increase in LHCD effectiveness.

In this Letter, we present an experimental observation of efficient lower hybrid current drive above the anomalous lower hybrid density limit in a diverted configuration. To the best of our knowledge, this is the first unambiguous report of efficient generation of noninductive current above $\bar{n}_e \approx 1 \times 10^{20}$ m^{-3} in this configuration. Our approach in the latest experimental campaign was to explore LHCD at high densities near the accessibility limit but at minimal Greenwald fraction. This was done by raising the plasma current further up to 1.4 MA under otherwise identical conditions. No special wall conditioning was found necessary to recover values of LHCD efficiency at high density that are consistent with the engineering efficiency scaling evaluated at low density.

The experiment presented in this Letter was carried out on Alcator C-Mod [17] (major radius $R = 67$ cm and minor radius $a = 22$ cm). We focus on the LH density limit observed in the L-mode plasmas without any additional heating schemes. Both the magnetic field ($B_t =$ 5–8 T) and the density ($\bar{n}_e < 1.5 \times 10^{20}$ m^{-3}), which govern the wave and boundary physics, correspond to those anticipated for a reactor. The lower hybrid current drive system [18] injects a high frequency rf wave ($f_0 = 4.6$ GHz) at power levels of up to 1 MW (injected). The interaction of the injected wave with the boundary plasma was monitored by measuring the wave frequency spectra with internal rf probes distributed around the tokamak. In particular, the inner-wall probe is ideally suited to observe a wave field that has undergone various wave-edge interactions on its first pass across the tokamak from the low-field side to the high-field side. Nonthermal electron cyclotron emission (ECE) and hard x-ray (HXR) bremsstrahlung emission are used to monitor fast electron generation by LHCD. The HXR diagnostic system [19] has 32 sight lines that view the poloidal cross section of the plasma with a detector at the outer midplane, providing information on the fast electron generation profile.

Figure 1 shows an example of a low-Greenwald fraction plasma with LHCD ($\bar{n}_e/n_G = 0.16$ with $I_p = 1.2$ MA) at a density above the nominal density limit. The line-averaged density was $\bar{n}_e = 1.3 \times 10^{20}$ m^{-3}. A net LH power of 600 kW was coupled to the plasma for 400 ms. The peak parallel refractive index launched was $n_{//} = 1.9$. As shown in Fig. 1(c), current drive is evidenced by reduction in loop voltage with the application of LH power, as the inductive drive required to maintain the prescribed plasma current is reduced in the presence of the fast electron tail [20]. This indicates that the LH power was effectively replacing a part of the Ohmic power, and the plasma current was partially driven noninductively. The central electron temperature remained at $T_{e,0} \approx 3$ keV, indicating that the change in loop voltage is not due to the change in resistivity. Figure 1(d) shows the correlated response of the edge nonthermal ECE with LHCD. Under similar conditions at low plasma current, the nonthermal emission is negligible.

The observed drop in the loop voltage is consistent with the rf current drive efficiency previously inferred on C-Mod. In our experiment, the fractional loop voltage drop is observed to be $\Delta V/V = 0.17$ with the injected

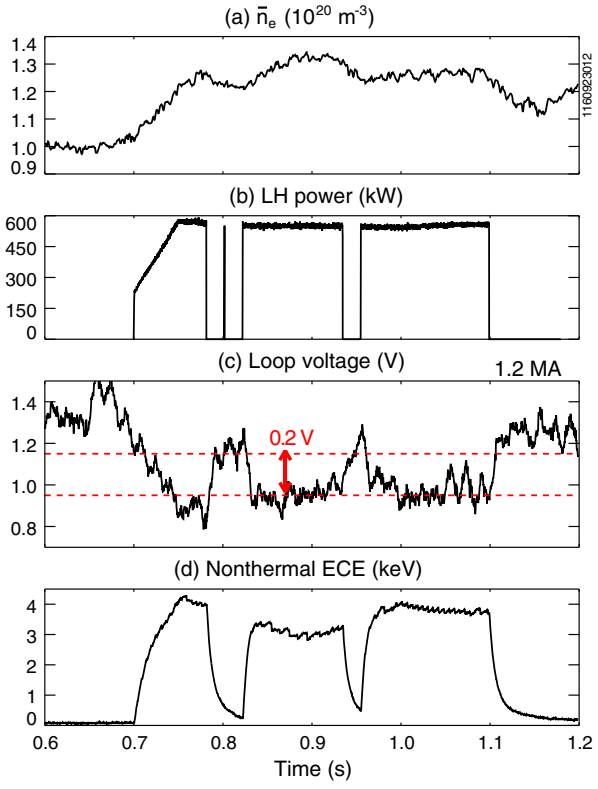

FIG. 1. Time traces of an 1.2 MA plasma with lower hybrid current drive. (a) Line-averaged density. (b) Injected LH power. (c) Loop voltage. (d) Nonthermal electron cyclotron emission.

power $x = P_{\mathrm{LH}}/(n_{e,19} I_p R_0) = 0.056\ (\mathrm{MW\,m^2\,MA^{-1}})$. This pair is found to be in line with the data set (Fig. 5 in Ref. [22]) that was used to evaluate the current drive efficiency in a low-density regime. In that study, $\Delta V/V$ was scanned as a function of the LH power, and it was fitted to a functional form [23] of $\Delta V/V = (\eta_0 + \eta_1)x/(1 + \eta_1 x)$ to infer the rf current drive efficiency: $\eta_0 = n_e I_p R_0/P_{\mathrm{LH}} \approx 2.5 \pm 0.2 (10^{19}\ \mathrm{MA\,MW^{-1}\,m^{-2}})$, and the hot conductivity term due to the presence of the dc field: $\eta_1 = 0.4 \pm 0.5$. Thus, the observed loop voltage drop consistent with the previous experimental data set shows that the experiment was limited by the injected power only.

Clear evidence for reduced parasitic wave-edge plasma interaction in this low-Greenwald fraction plasma is provided by measurements of the frequency spectrum by an inner-wall probe. Figure 2 compares the LH frequency spectra in low- and high-Greenwald fraction plasmas (0.16 vs 0.36) at fixed $\bar{n}_e = 1.3 \times 10^{20}\ \mathrm{m^{-3}}$ under otherwise identical conditions. The lower current (higher Greenwald fraction) discharges typically show a pump-wave amplitude that is lower by about 10 dB [13] at this location, suggesting that first pass losses might be an important player in the LH density limit behavior. The symmetrically broadened frequency components around the source frequency indicate a role of turbulence scattering [24] and/or ion sound PDIs [25]. In addition, the harmonics of the sideband below the source frequency evidences the onset of ion cyclotron PDIs [6].

On the other hand, in a low-Greenwald fraction plasma that exhibits a good current drive efficiency, experimental signatures of parasitic wave-edge interactions are largely eliminated despite exhibiting the same line-averaged density. A level of pump broadening is noticeably reduced, which can be attributed to a reduction in blobby transport occurring in the SOL. It was previously reported [26] that the effective particle diffusion coefficient ($D_{\mathrm{eff}} = \Gamma/\nabla n_e$, where Γ is the particle flux) in the near SOL is reduced significantly below $\bar{n}_e/n_G \approx 0.2$ with corresponding reduction in density shoulder in the far SOL. Under this condition, the launched wave is not expected to undergo significant scattering interactions with the background turbulence.

Furthermore, the suppressed PDI sidebands indicate that the nonlinear wave scattering process is also below the threshold condition, consistent with a homogeneous PDI analysis [27]. The reasoning for this is as follows: based on previous SOL profile measurements [13], the SOL density at such a low-Greenwald fraction plasma quickly falls to below $n_e \approx 0.3 \times 10^{20}\ \mathrm{m^{-3}}$ outside the separatrix without forming a shoulder structure even at $\bar{n}_e = 1.3 \times 10^{20}\ \mathrm{m^{-3}}$. At this local density, a PDI analysis shows that the convective threshold condition ($\gamma \Delta t > \pi$) is not satisfied for the most unstable ion mode of $n_{//} \sim 20$ in the limit of perpendicular coupling. Here, γ is the growth rate, and $\Delta t = \Delta y/v_{g\perp}$ is the residence time of the excited sideband LH wave within the pump-wave resonance cone determined by the height of a single grill structure ($\Delta y = 6$ cm) and the sideband perpendicular group velocity ($v_{g\perp} \approx (\omega/k_{\|})(\omega/\omega_{pe})$). Note that SOL temperature is not found to be a strong function of the Greenwald fraction. It is also a weak function of the power to the SOL ($T_e \sim P_{\mathrm{SOL}}^{2/7}$). Therefore, the edge and/or SOL density and its associated density fluctuation level are found to be an important parameter to control parasitic wave interactions at the plasma edge.

Fast electron generation is found to be increased by more than 2 orders of magnitude in the high current plasmas compared to the lowest current cases (0.55 MA). Figure 3 summarizes HXR count rate observations as a function of

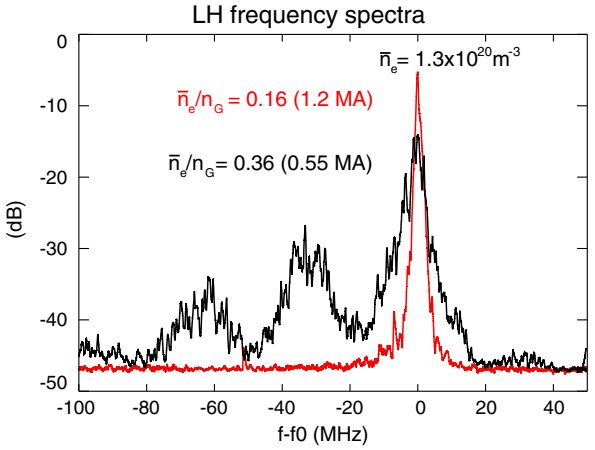

FIG. 2. LH frequency spectra measured with an inner-wall probe at $\bar{n}_e/n_G = 0.16$ ($I_p = 1.2$ MA, $P_{\mathrm{LH}} = 600$ kW) in red and 0.36 ($I_p = 0.55$ MA, $P_{\mathrm{LH}} = 300$ kW) in black. In both cases, $\bar{n}_e \approx 1.3 \times 10^{20}\ \mathrm{m^{-3}}$.

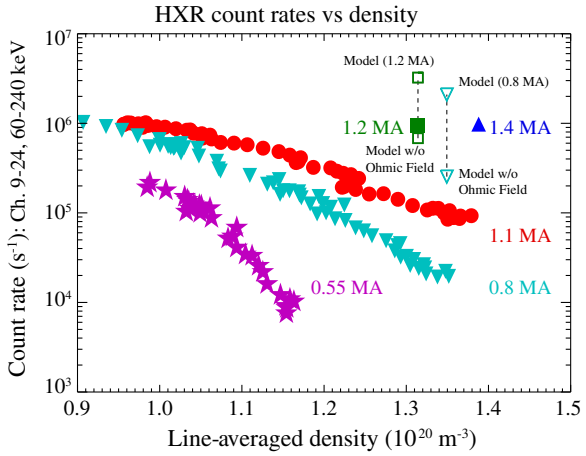

FIG. 3. Hard x-ray line-integrated count rates as a function of $\bar{n}_e$ at different currents: 0.55 (star), 0.8 (inverted triangle), 1.1 (circle), 1.2 (square), and 1.4 MA (triangle). Data are calibrated against the detector shielding thicknesses and the coupled LH powers. Two unfilled square (inverted triangle) symbols denote the modeled count rates of the 1.2 MA (0.8 MA) discharge with and without the dc electric field.

the line-averaged density at different currents. The HXR emission may be taken as a proxy for fast electron generation. The count rates are summed from 16 central viewing chords out of 32 chords in the energy range from 60 to 240 keV. While previous experimental results at lower plasma current exhibit an exponential decay of HXR emission with increasing density, the count rates at $I_p > 1$ MA are substantially higher for $\bar{n}_e > 1 \times 10^{20}$ m^{-3}. The loop voltages in these plasmas remain similar at about 1.0 V, eliminating the possibility that a higher dc electric field could have accelerated the fast electrons more in a high-current plasma.

Figure 4 compares the HXR count rates versus the channel number between the low-current and high-current plasmas. In the low-current cases, the profile is peaked at the central chord. This feature was proposed to be caused by the modification in the launched spectrum due to wave-edge plasma interactions [14,28], which is in line with our experimental observation of the increased wave interaction with the edge plasma with increased Greenwald fraction at the fixed line-averaged density. In the high-current cases, the fast electron generation profile is not peaked, indicating the broadening of wave power deposition. While such a broadening with increasing current is generally attributed to the increase in core temperature and an increased level of poloidal up-shift, our result suggests that this current dependence might not be fully isolated from the change in the edge-SOL plasma with the decrease in the Greenwald fraction.

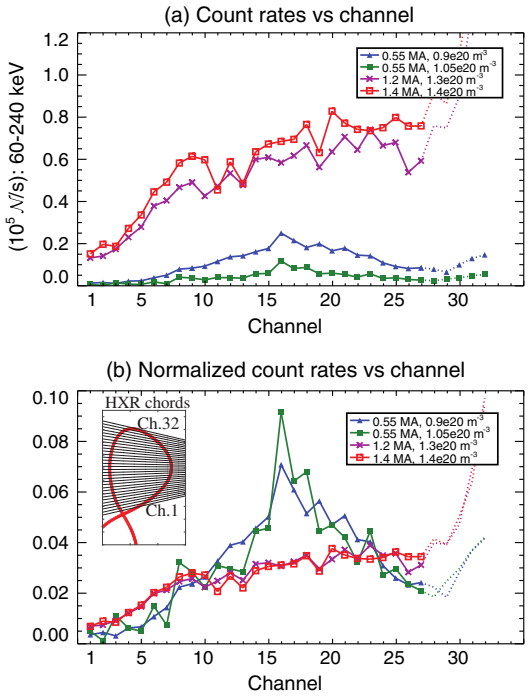

FIG. 4. (a) Hard x-ray count rates and (b) the normalized count rates to the total count rates as a function of the channel number. The profile in blue (green) is measured in a plasma with $I_p = 0.55$ MA at $\bar{n}_e \approx 0.9(1.05) \times 10^{20}$ m^{-3}. The profile in purple (red) is measured in a plasma with $I_p = 1.2(1.4)$ MA and $\bar{n}_e \approx 1.3(1.4) \times 10^{20}$ m^{-3}. (Inset) The 32 sight lines of the HXR diagnostic system, with the LCFS of the 1.2 MA discharge overlaid in red. The increasing count rates observed for the channels greater than the no. 28 could be due to thick target bremsstrahlung emission outside the LCFS [12].

The increased level of the HXR count rates observed is in reasonable agreement with preliminary steady-state GENRAY-CQL3D model calculations [29,30] shown in Fig. 3, which includes a simple exponentially decaying SOL for the temperature and density profiles outside the separatrix with a fixed scale length normalized to a minor radius of $\lambda = 0.022$. About 20% of the LH power is found to be collisionally lost in the model. Because of the known sensitivity of the simulated total driven current to the dc electric field [31], two simulations with and without the dc electric field were conducted. First, the dc electric field is assumed to have a $1/R$ dependence with the on-axis value of $E_0 = 0.234$ V/m, consistent with the measured loop voltage of 1 V. The predicted total current (1.23 MA) is found to agree well with the experimental current (1.2 MA), while the predicted hard x-ray count rates ($=3.3 \times 10^6$ $\mathcal{N}$/s) are higher by a factor of 3 than the experimental measurement (Fig. 3). The second simulation result without the dc electric field predicts the count rates of 0.69×10^6 $\mathcal{N}$/s, which is below the experimental count rates. The rf driven current is predicted to be 86 kA. Since the experimental count rates are between the two modeling results, it is concluded that the ray-tracing–Fokker-Planck model can reasonably reproduce the observed experimental level of the HXR emission. Note that this standard model is found to significantly overpredict the count rates in the low-current case (e.g., 800 kA), as shown in Fig. 3. It has been reported [11,14] that a proper modeling of the diverted SOL plasma (e.g., the shoulder structure) and associated parasitic wave interactions is crucial in reproducing the strong reduction in the count rates observed in the low-current cases. An agreement found in the high-current case supports that wave parasitic losses in the boundary plasma are largely eliminated in the low-Greenwald fraction plasma. Further investigations are necessary in modeling the fast electron population in the presence of a strong dc electric field.

In summary, efficient lower hybrid current drive is recovered on the Alcator C-Mod tokamak up to the accessibility limit when $\bar{n}_e/n_G < 0.2$. The dependence of SOL parameters on Greenwald density fraction is identified as an important tool that can be used to control edge-SOL plasma conditions and attain efficient LHCD above the nominal LH density limit. The observed change in the loop voltage is in line with the efficiency evaluated at a low density. Several orders of magnitude increase in the fast electron generation is indicated by HXR observations, which is consistent with initial ray-tracing–Fokker-Planck

synthetic-diagnostic analysis. The frequency spectra measurements detect parasitic wave interactions with the edge plasma, whose suppression is correlated with the improvement in LHCD efficiency.

Further work remains to identify more clearly the dominant mechanisms for the observed loss of efficiency in plasmas with an increased Greenwald fraction. In particular, an experiment in a strong single-pass damping regime would be particularly helpful for this purpose in order to assess the loss occurring on the first pass. A high temperature in a reactor is expected to suppress collisions and PDIs. The insight that SOL conditions play such a key role suggests a number of pathways forward to attain an efficient LHCD in reactor—akin to the realization that the Greenwald density limit itself may be overcome by proper tailoring of the edge and pedestal density profiles [32–34]. Unlike our experiments, the Greenwald fraction in a fusion reactor is fixed and cannot be lowered. However, high-field tokamak reactors that can operate at a moderate Greenwald fraction [35] may provide a favorable SOL condition for wave penetration. Furthermore, a placement of the launcher at the high-field side (HFS) of the tokamak in a double null configuration [36] may offer another important optimization approach via magnetic balance control. In this magnetic configuration, the HFS SOL becomes disconnected from the low-field-side SOL, and density shoulders and blobby transport phenomena are expected to be absent there, as indicated by the HFS SOL profile measurements on Alcator C-Mod [37]. In this situation, parasitic wave interactions may be avoided even at high-Greenwald fraction.

The authors thank the entire Alcator C-Mod team for their support in carrying out the LHCD experiment. This research was conducted on Alcator C-Mod, a DOE Office of Science User Facility, and is supported by DOE Contract No. DE-FC02-99ER54512.

*Corresponding author.
sgbaek@psfc.mit.edu

[1] N. J. Fisch, Phys. Rev. Lett. **41**, 873 (1978).
[2] N. J. Fisch and A. H. Boozer, Phys. Rev. Lett. **45**, 720 (1980).
[3] P. T. Bonoli, Phys. Plasmas **21**, 061508 (2014).
[4] W. Hooke, Plasma Phys. Controlled Fusion **26**, 133 (1984).
[5] M. Brambilla, Nucl. Fusion **19**, 1343 (1979).
[6] M. Porkolab, S. Bernabei, W. M. Hooke, R. W. Motley, and T. Nagashima, Phys. Rev. Lett. **38**, 230 (1977).
[7] Y. Takase, M. Porkolab, J. J. Schuss, R. L. Watterson, C. L. Fiore, R. E. Slusher, and C. M. Surko, Phys. Fluids **28**, 983 (1985).
[8] R. Cesario, L. Amicucci, A. Cardinali, C. Castaldo, M. Marinucci, L. Panaccione, F. Santini, O. Tudisco, M. L. Apicella, G. Calabrò *et al.*, Nat. Commun. **1**, 55 (2010).
[9] M. Goniche, V. Basiuk, J. Decker, P. K. Sharma, G. Antar, G. Berger-By, F. Clairet, L. Delpech, A. Ekedahl, J. Gunn *et al.*, Nucl. Fusion **53**, 033010 (2013).
[10] B. J. Ding, E. H. Kong, M. H. Li, L. Zhang, W. Wei, M. Wang, H. D. Xu, Y. C. Li, B. L. Ling, Q. Zang *et al.*, Nucl. Fusion **53**, 113027 (2013).
[11] G. M. Wallace, R. R. Parker, P. T. Bonoli, A. E. Hubbard, J. W. Hughes, B. L. LaBombard, O. Meneghini, A. E. Schmidt, S. Shiraiwa, D. G. Whyte *et al.*, Phys. Plasmas **17**, 082508 (2010).
[12] G. M. Wallace, A. E. Hubbard, P. T. Bonoli, I. C. Faust, R. W. Harvey, J. W. Hughes, B. L. LaBombard, O. Meneghini, R. R. Parker, A. E. Schmidt *et al.*, Nucl. Fusion **51**, 083032 (2011).
[13] S. G. Baek, R. R. Parker, P. T. Bonoli, S. Shiraiwa, G. M. Wallace, B. LaBombard, I. C. Faust, M. Porkolab, and D. G. Whyte, Nucl. Fusion **55**, 043009 (2015).
[14] S. Shiraiwa, S. G. Baek, I. Faust, G. Wallace, P. Bonoli, O. Meneghini, R. Mumgaard, R. Parker, S. Scott, R. W. Harvey *et al.*, AIP Conf. Proc. **1689**, 030016 (2015).
[15] I. C. Faust, D. Brunner, B. LaBombard, R. R. Parker, J. L. Terry, D. G. Whyte, S. G. Baek, E. Edlund, A. E. Hubbard, J. W. Hughes *et al.*, Phys. Plasmas **23**, 056115 (2016).
[16] B. Labombard, J. W. Hughes, N. Smick, A. Graf, K. Marr, R. McDermott, M. Reinke, M. Greenwald, B. Lipschultz, and J. L. Terry, Phys. Plasmas **15**, 056106 (2008).
[17] M. Greenwald *et al.*, Phys. Plasmas **21**, 110501 (2014).
[18] P. T. Bonoli *et al.*, Fusion Sci. Technol. **51**, 401 (2007).
[19] J. Liptac, R. Parker, V. Tang, Y. Peysson, and J. Decker, Rev. Sci. Instrum. **77**, 103504 (2006).
[20] Note that the current relaxation time [21] for the given plasma is $\tau_{CR} = 1.4a^2T_e^{3/2}/Z_{eff} = 230$ ms for $a = 0.22$ m, $T_e = 3$ keV and $Z_{eff} = 1.5$. Therefore, the current profile was not expected to be fully relaxed due to the tripping in the injected power.
[21] D. R. Mikkelsen, Phys. Fluids B **1**, 333 (1989).
[22] P. T. Bonoli, J. Ko, R. Parker, A. E. Schmidt, G. Wallace, J. C. Wright, C. L. Fiore, A. E. Hubbard, J. Irby, E. Marmar *et al.*, Phys. Plasmas **15**, 056117 (2008).
[23] G. Giruzzi, E. Barbato, S. Bernabei, and A. Cardinali, Nucl. Fusion **37**, 673 (1997).
[24] P. L. Andrews and F. W. Perkins, Phys. Fluids **26**, 2546 (1983).
[25] Y. Takase and M. Porkolab, Phys. Fluids **26**, 2992 (1983).
[26] B. LaBombard, R. L. Boivin, M. Greenwald, J. Hughes, B. Lipschultz, D. Mossessian, C. S. Pitcher, J. L. Terry, S. J. Zweben, and A. Group, Phys. Plasmas **8**, 2107 (2001).
[27] M. Porkolab, Phys. Fluids **20**, 2058 (1977).
[28] Y. Peysson, J. Decker, E. Nilsson, J. F. Artaud, A. Ekedahl, M. Goniche, J. Hillairet, B. Ding, M. Li, P. T. Bonoli *et al.*, Plasma Phys. Controlled Fusion **58**, 044008 (2016).
[29] A. P. Smirnov, R. W. Harvey, and K. Kupfer, Bull. Am. Phys. Soc. **39**, 1626 (1994), Abstract 4R11, http://flux.aps.org/meetings/YR9394/BAPSDPP94/4r0.html.
[30] R. W. Harvey and M. C. McCoy, in *Proceedings of the IAEA Technical Committee Meeting on Advances in Simulation and Modeling of Thermonuclear Plasmas, Montreal, 1992* (IAEA, Vienna, 1993), p. 489.
[31] F. M. Poli, P. T. Bonoli, M. Chilenski, R. Mumgaard, S. Shiraiwa, G. M. Wallace, R. Andre, L. Delgado-Aparicio,

S. Scott, and J. R. Wilson, Plasma Phys. Controlled Fusion **58**, 095001 (2016).
[32] P. T. Lang, W. Suttrop, E. Belonohy, M. Bernert, R. M. Mc Dermott, R. Fischer, J. Hobirk, O. Kardaun, G. Kocsis, and B. Kurzan, Nucl. Fusion **52**, 023017 (2012).
[33] T. H. Osborne, A. W. Leonard, M. A. Mahdavi, M. Chu, M. E. Fenstermacher, R. La Haye, G. McKee, T. W. Petrie, E. Doyle, and G. Staebler, Phys. Plasmas **8**, 2017 (2001).
[34] H. Zohm, C. Angioni, E. Fable, G. Federici, G. Gantenbein, T. Hartmann, K. Lackner, E. Poli, L. Porte, and O. Sauter, Nucl. Fusion **53**, 073019 (2013).
[35] B. N. Sorbom, J. Ball, T. R. Palmer, F. J. Mangiarotti, J. M. Sierchio, P. Bonoli, C. Kasten, D. A. Sutherland, H. S. Barnard, C. B. Haakonsen *et al.*, Fusion Eng. Des. **100**, 378 (2015).
[36] B. LaBombard, E. Marmar, J. Irby, J. L. Terry, R. Vieira, G. Wallace, D. G. Whyte, S. Wolfe, S. Wukitch, S. Baek *et al.*, Nucl. Fusion **55**, 053020 (2015).
[37] B. LaBombard, J. E. Rice, A. E. Hubbard, J. W. Hughes, M. Greenwald, J. Irby, Y. Lin, B. Lipschultz, E. S. Marmar, C. S. Pitcher *et al.*, Nucl. Fusion **44**, 1047 (2004).